GEODEZJA I KARTOGRAFIA
GEODESY AND CARTOGRAPHY
Vol. 54, No 4, 2005, pp. 177-189

A new marine geoid model for Argentina combining altimetry, shipborne gravity data and CHAMP/GRACE-type EGMs

Claudia Tocho [1], Georgios S. Vergos [2], Michael G. Sideris [3]

[1] Facultad de Ciencias Astronómicas y Geofisicas
Paseo del Bosque s/n, 1900 La Plata, Argentina
e-mail: ctocho@fcaglp.unlp.edu.ar
[2] Department of Geodesy and Surveying, Aristotle University of Thessaloniki
Univ. Box. 440, 54124 Thessaloniki, Greece
e-mail: vergos@topo.auth.gr
[3] Department of Geomatics Engineering, University of Calgary
2500 University Drive N.W., Calgary, Alberta, T2N 1N4, Canada
e-mail: sideris@ucalgary.ca

Received: 4 October 2005/Accepted: 20 December 2005

Abstract: Marine geoid modelling in the Atlantic coastal region of Argentina is problematic. Firstly, because of the insufficient amount of available shipborne gravity data, which renders a purely gravimetric solution not feasible. Secondly, because of the very strong ocean currents, that affect the quality of satellite altimetry data, so that a purely altimetric model is too noisy, even after low-pass filtering the Sea Surface Heights (SSHs) to remove (part of) the influence of the oceanographic signals. Thus, the recommended solution is to employ a combination method and the use of all the available gravity and altimetry data together. This is a suitable solution since (i) combination methods such as least squares collocation and Input Output System Theory (IOST) inherently low-pass filter and weigh the data, and (ii) will make use of the altimetric heights to fill the gaps of the shipborne gravity data. Following this idea, purely altimetric, gravimetric and combined (using the IOST method) marine geoid models have been estimated for Argentina, employing all available shipborne gravity data, satellite altimetry SSHs and the latest Earth Gravity Models (EGMs) developed from CHAMP and GRACE missions. The new EGMs are especially useful to assess the quality of the new geoid models, especially against EGM96, which was used in an older ERS1-only solution for the same area. From the comparison of the estimated geoid models with respect to stacked TOPEX/Poseidon SSHs, the authors found that the altimetric model provides the best agreement while the combined one improves the accuracy (1σ) of the gravimetric solution.

Keywords: Marine geoid, altimetry, shipborne gravity, IOST, "combined" EGM, GRACE, CHAMP

1. Introduction

Continuing authors' prior investigation (Tocho et al., 2005), carried out in order to determine a high-accuracy and high-resolution geoid model for the Atlantic coastal region of Argentina, recent study is focussed on the improvement of previously obtained results using a "combined" geopotential model (EGM) derived from the latest CHAMP

(CHAllenging Minisatellite Payload) and GRACE (Gravity Recovery and Climate Experiment) (Vergos et al., 2004). It should be mentioned that this so-called "combined" EGM is not a new model determined from raw CHAMP and GRACE data, but a combination of the harmonic coefficients of the latest EGMs from GFZ (GeoForschungs-Zentrum Potsdam) and the Center of Space Research (CSR), University of Texas. Therefore, by inspecting the CHAMP and GRACE degree variances and their errors, the model more accurate for different harmonic degrees was defined, and then a "combined" EGM was developed, using the CHAMP EGM for n = 2–7, the GRACE EGM for n = 8–120, and EGM96 for n = 121–360 (Vergos et al., 2004).

In the present study, pure gravimetric and altimetric geoid models as well as a combined solution using the Multiple Input Multiple Output System Theory (MIMOST) method (Sideris, 1996; Andritsanos and Tziavos, 2002; Vergos et al., 2005a) have been estimated.

Pure gravimetric and altimetric geoid models are single data source ones, i.e. they are computed from shipborne gravity and satellite altimetry data alone, respectively. A combined solution on the other hand, makes use of both data types. The latter solution was computed to investigate if the combined use of satellite altimetry and shipborne data will improve the estimated geoid model compared to the purely gravimetric one.

The area of investigation covers the eastern part of Argentina bounded between $-34° \leq \varphi \leq -55°$ and $290° \leq \lambda \leq 304°$; it is mainly a marine area that includes Falkland Islands.

The marine gravity data available were gravity anomalies provided by the Bureau Gravimétrique International (BGI, 2001). Since there were some gaps between the ship tracks, the KMS01 and the newest release KMS02, $2' \times 2'$ altimetry-derived free-air gravity anomalies (Andersen and Knudsen, 1998) have been used as fill in information. KMS02 is the newest compilation of a global altimetry-derived marine free-air gravity field by the KMS group at the National Danish Survey and Cadastre (Andersen et al., 2005).

The topographic/bathymetric data for the residual terrain model (RTM) reduction (Forsberg, 1984) were those of the Smith and Sandwell model (Smith and Sandwell, 1997), which resulted as a combination of depths derived from altimetry and echo soundings.

To derive geoid heights from altimetric measurements, the necessary information on quasi-stationary sea surface topography (QSST) was computed from the Dynamic Ocean Topography (DOT) model, EGM96.DOT model, which is a spherical harmonic expansion of the SST, complete to degree and order 20 (Lemoine et al., 1998). That model was derived during the simultaneous adjustment for the development of the EGM96 geopotential model.

Finally, the altimetric data consist of sea surface heights (SSHs) from the Geodetic Mission ERS1 GM and repeated TOPEX/POSEIDON (T/P) SSHs from the entire 3rd year of the satellites mission (AVISO, 1998).

2. Geoid modelling

2.1. Altimetric geoid with ERS1 data

An altimetric satellite measures the time taken by a radar pulse to travel from the satellite to the sea surface and back to the satellite receiver. Combined with precise satellite location data, altimetry measurements yield Sea Surface Heights (SSHs), i.e. the height of the sea above a reference ellipsoid of revolution. The derived SSHs must be corrected for several geophysical effects (tides, tidal loading, ionosphere, wet and dry troposphere, inverse barometer and electromagnetic bias) and instrumental errors (ultra-stable oscillator, centre of gravity, corrections for instrument and algorithm effects that can not be modelled, and for waveforms). After applying those corrections, Corrected Sea Surface Heights (CorSSHs) are available for the Geodetic Mission of ERS1.

The altimetric geoid was computed using 70510 CorSSHs from the ERS1 Geodetic Mission, which were obtained by applying all instrumental and geophysical corrections to the raw SSHs provided by AVISO (1998). Those corrections were computed using the available algorithms and models provided by AVISO itself. Table 1 presents the statistics of the 70510 corrected ERS1-GM SSHs for the area under study.

Sea Surface Heights contain information about both the geoid and the sea surface topography (SST); while the latter consists of a time-dependent and a nearly time-independent component (quasi-stationary part). Stacking the repeat tracks can eliminate the effect of the time-dependent component and part of the sea surface variability effects that influence the data. The corrected sea surface heights were then reduced from the MSS to the geoid for the QSST signal, which is the quasi-stationary part of Sea Surface Topography. This was performed by estimating the QSST at each sub-satellite point (QSST in CorSSHs) and removing the contribution of the QSST from the corrected sea surface height value (CorSSHs – QSST). The quasi-stationary component of the SST is modelled by a spherical harmonic series of the Dynamic Ocean Topography (DOT) EGM96.DOT model (Table 1). Table 1 shows also the statistics of the QSST in the investigated area as well as the CorSSHs after removing the QSST.

The altimetric geoid model was then computed using a remove-compute-restore procedure, i.e. by first removing the contribution of the new combined geopotential model (N^{GMcomb}) from the corrected sea surface heights and then RTM-reducing to take into account the effect of bathymetric masses to the geoid signal (N^{RTM}). The statistics of the geoid referenced to the new "combined" EGM (CorSSHs – QSST – N^{GMcomb}) as well as those of the residual geoid heights after the residual terrain model (RTM) reduction (CorSSHs – QSST – N^{GMcomb} – N^{RTM}) are given in Table 1. The residual geoid heights in Table 1 indicate that some values may still contain blunders and/or systematic errors. Therefore, a simple three root mean square (3 rms) test was performed for blunder detection, and a total of 438 points were removed.

The residual Sea Surface Heights after the 3 rms test (N_{res}) represent the medium wavelengths of the geoid heights and can be used to compute the subsequent altimetric geoid solution. Point residual geoid heights (N_{res}) were gridded with a weighted means method with prediction power two on a grid of $3' \times 3'$. The gridding of the random distributed data was based on a weighted means method using the inverse of the square of the distance as the weight for each irregular observation. It was done using the *geogrid* program from the GRAVSOFT software (Tscherning et al., 1992). The statistics of the gridded ERS1 residual geoid heights with no filter applied (N_{res} (no filtering)) is given in Table 1.

T a b l e 1. Statistics of the ERS1-GM altimetric geoid processing [m]

Remove step	Min	Max	Mean	σ
70510 ERS1-GM CorSSHs	0.589	19.010	11.259	±3.079
QSST in CorSSHs	−0.692	0.083	−0.169	±0.128
CorSSHs − QSST	0.772	19.646	11.428	±3.081
N^{GMcomb}	1.112	18.889	11.075	±2.907
CorSSHs − QSST − N^{GMcomb}	−1.337	2.922	0.352	±0.338
N^{RTM}	−0.557	0.847	0.070	±0.158
CorSSHs − QSST − N^{GMcomb} − N^{RTM}	−1.361	2.892	0.282	±0.336
3 rms test for blunders detection ⇒ 438 points removed				
N_{res} = CorSSHs − DOT − N^{GMcomb} − N^{RTM}	−1.266	1.316	0.273	±0.314
Gridding				
N_{res} (no filtering)	−1.036	1.285	0.276	±0.274
Area with very high SSV; the gridded N_{res} was low-pass filter with a cut-off frequency of 22 km				
N_{res} (ω_c = 22 km)	−1.118	0.838	0.068	±0.253
Restore step	**Min**	**Max**	**Mean**	σ
N^{GMcomb}	1.102	19.166	11.231	±2.874
N^{RTM}	−0.567	0.847	0.070	±0.153
N_{alt}	**0.794**	**19.384**	**11.368**	**±3.018**

Due to a very high Sea Surface Variability (SSV) present in the residual field, the data was low-pass filtered with a Wiener-type of filter, empirically testing different cut-off frequencies ω_c. The selection of the cut-off frequency to be used was based on a maximum noise reduction with the minimum signal loss principle. Finally a cut-off frequency corresponding to ω_c = 22 km was selected for the low-pass filtering procedures using a collocation-type of filter, assuming Kaula's rule for the geoid spectrum. The final altimetric geoid solution (N_{alt}) was obtained by restoring the geopotential model (N^{GMcomb}) and adding the contribution of the bathymetry (N^{RTM}).

2.2. Gravimetric geoid solution

The gravimetric geoid model was computed using 12823 shipborne free-air gravity anomalies provided by the Bureau Gravimétrique International (BGI) as referred to the Geodetic Reference System 1967 (GRS67). The data was then transformed to the Geodetic Reference System 1980 (GRS80) in order to become compatible with the altimetric data (Li and Sideris, 1997), and then converted into free-air gravity anomalies using the QSST values from the EGM96. DOT 16961 altimetry-derived gravity anomalies from the KMS01 and KMS02 global datasets were used to fill in the sparse coverage of shipborne gravity measurements offshore Argentina. The evaluation of these two global models in the investigated area will be presented in the next section. Distribution of the gravity data used is shown in Fig. 1.

The computation of the gravimetric geoid model was based on the classical remove-compute-restore technique. First, the contribution of the new "combined EGM" was removed, and then the bathymetry was taken into account using an RTM reduction. The difference with the altimetric geoid determination is due to the fact that after the residual gravity anomalies were gridded the contribution of the bathymetry was restored prior the geoid height prediction (Dahl and Forsberg, 1998). The computation of residual gravimetric geoid heights was carried out by applying two-dimensional FFT approximate Stokes convolution on the $3' \times 3'$ grid (Strang van Hees, 1990) using the *fftgeoid* program (Li, 1993).

$$N_{res} = \frac{R \Delta\varphi \Delta\lambda}{4\pi\gamma} \mathrm{F}^{-1}\{\{\mathrm{F}\{\Delta g \cos\varphi\}\, \mathrm{F}(\Delta\varphi, \Delta\lambda, \varphi_m)\}\} \tag{1}$$

where N_{res} is the estimated residual gravimetric geoid height, and F, F^{-1} denote the direct and inverse 2D Fourier transforms, respectively. Final gravimetric geoid solutions were computed by restoring the contribution of the geopotential model.

The statistics of the gravimetric geoid processing using the KMS01 and KMS02 datasets are presented in Tables 2 and 3, respectively.

Table 2. Statistics of gravimetric geoid model processing with KMS01 data

Remove step [mGal]	Min	Max	Mean	σ
Δg_{FA}	−133.03	142.57	3.49	±22.71
Δg^{GMcomb}	−112.91	114.16	1.92	±21.37
$\Delta g_{FA} - \Delta g^{GMcomb}$	−80.61	63.21	1.57	±9.46
Δg^{RTM}	−34.11	32.98	0.28	±3.58
$\Delta g_{red} = \Delta g_{FA} - \Delta g^{GMcomb} - \Delta g^{RTM}$	−54.98	61.78	1.29	±9.32
3 rms test for blunders detection ⇒ 653 points removed				
$\Delta g_{red} = \Delta g_{FA} - \Delta g^{GMcomb} - \Delta g^{RTM}$	−28.23	28.20	1.42	±7.65
Δg_{red} ⇒ gridding on $3' \times 3'$ grid				
Δg_{red} grid	−27.92	27.62	0.99	±7.11
Δg^{RTM}	−34.30	35.88	0.53	±4.35
Δg_{res} grid = Δg_{red} grid + Δg^{RTM} grid	−35.20	46.68	1.51	±7.40
Residual geoid heights computed ⇒ 2D FFT spherical Stokes kernel convolution (Strang van Hees, 1990) computed with integration radius ~ 10 km				
N_{res} [m]	−0.445	0.408	0.013	±0.076
Restore step [m]	**Min**	**Max**	**Mean**	σ
N^{GMcomb}	1.102	19.166	11.231	±2.874
N_{grav}	1.079	19.079	11.249	±2.869

Table 3. Statistics of gravimetric geoid model processing with KMS02 data

Remove step [mGal]	Min	Max	Mean	σ
Δg_{FA}	−133.03	142.57	3.70	±22.74
Δg^{GMcomb}	−112.91	114.16	1.92	±21.37
$\Delta g_{FA} - \Delta g^{GMcomb}$	−80.61	63.21	1.78	±9.59
Δg^{RTM}	−34.11	32.98	0.28	±3.58
$\Delta g_{red} = \Delta g_{FA} - \Delta g^{GMcomb} - \Delta g^{RTM}$	−54.98	61.78	1.50	±9.44
3 rms test for blunders detection $\Rightarrow$ 575 points removed				
$\Delta g_{red} = \Delta g_{FA} - \Delta g^{GMcomb} - \Delta g^{RTM}$	−29.78	29.76	1.60	±7.93
$\Delta g_{red} \Rightarrow$ gridding on $3' \times 3'$ grid				
Δg_{red} grid	−29.27	28.99	1.03	±7.31
Δg^{RTM}	−34.30	35.88	0.53	±4.30
Δg_{res} grid = Δg_{red} grid + Δg^{RTM} grid	−46.68	49.59	1.56	±7.56
Residual geoid heights computed $\Rightarrow$ 2D FFT spherical Stokes kernel convolution (Strang van Hees, 1990) computed with integration radius ~ 10 km				
N_{res} [m]	−0.445	0.406	0.014	±0.078
Restore step [m]	**Min**	**Max**	**Mean**	σ
N^{GMcomb}	1.102	19.166	11.231	±2.873
N_{grav}	1.079	19.096	11.245	±2.869

2.2.1. *Validation of KMS01 and KMS02 altimetry-derived free-air gravity anomalies*

KMS01 and KMS02 altimeter-derived gravity anomaly grids offshore Argentina were compared with one another and with ship-track gravity anomalies computed from the BGI gravity database.

KMS02 is the newest release of the KMS global marine free-air gravity field (Andersen et al., 2005). $2' \times 2'$ KMS grids of gravity anomalies have been computed via conversion of marine geoid heights using the inverse Stokes's formula. Sub-grids were extracted from the grids over the study area. The statistics of the gravity anomalies for each grid, after terrestrial gravity anomalies were removed using the *grdlandmask* option in the Generic Mapping Tools (GMT) (Wessel and Smith, 1998); it is given in Table 4.

Table 4. Statistics of KMS01 and KMS02 grids, their differences and ship-tracks gravity anomalies offshore Argentina [mGal]

	Min	Max	Mean	σ
KMS01	−137.57	130.77	4.41	±25.59
KMS02	−134.26	131.47	4.39	±25.90
Shipborne data	−133.03	142.57	4.01	±28.64
KMS02-KMS01	−41.37	64.17	−0.02	±4.15

First three rows of Table 4 show that the statistics of both KMS models are similar; they also show that the range of shipborne gravity anomalies is comparable. The last row shows the statistics of the differences between KMS02 and KMS01. Those differences are also presented in Fig. 2.

The larger differences occur over the South American-Scotia plate boundary and the edge of the continental shelf of Argentina. The KMS gravity anomalies were interpolated to the locations of the shipborne data using a bilinear function.

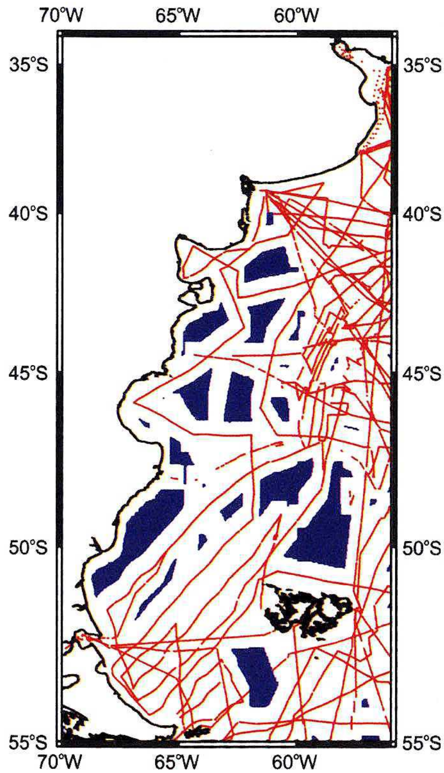

Fig. 1. Gravity data distribution

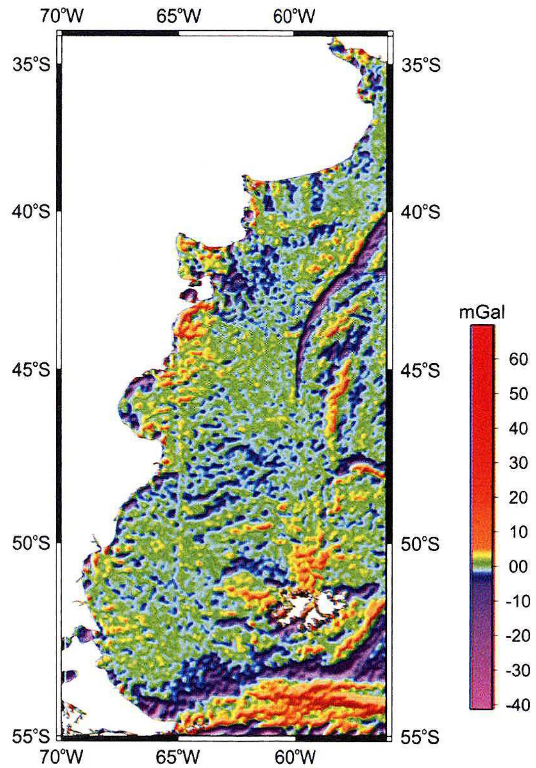

Fig. 2. KMS02-KMS01 in Argentina

Table 5 presents the statistics of the differences between both grids and 12823 shipborne gravity points obtained using the *geoip* program from the GRAVSOFT software (Tscherning et al., 1992). Plotting the differences between two different KMS grids and the shipborne marine gravity anomalies, one can conclude that the large differences correspond to the same ship-tracks. Due to the uncertain quality of the ship-track data, they should be used with caution to provide any reliable indication of the quality of the altimeter grids.

Table 5. Statistics of the differences between KMS grids and the shipborne marine gravity anomalies [mGal]

	Min	Max	Mean	σ
KMS01 – shipborne	−61.47	67.74	0.99	±10.31
KMS02 – shipborne	−63.67	66.31	1.25	±9.99

2.3. Combined solution using MIMOST

The estimation of the combined geoid solution was carried out using the MIMOST method in a smaller area between 40°S to 50°S in latitude and 294°E to 304°E in longitude. The inputs to MIMOST were two kinds of residual gravimetric geoid heights (one with shipborne gravity data filled in with KMS01 data and the other filled in with KMS02 data) and the residual altimetric geoid heights, prior to the contribution of the geopotential model was restored in order to avoid long wavelength errors. Since no information available exists on the input errors of both the altimetric and gravimetric models, that are necessary to apply the MIMOST method, a simulated noise is used as input errors (Vergos et al., 2005b). The input errors for each dataset (white noise) were generated using the σ = 19 cm for the altimetric geoid heights and σ = 21 cm for the gravimetric solutions. The final solution from the combined method as well the output error Power Spectrum Density (PSD) function were estimated according to the following equations:

$$\hat{X}_0 = \hat{H}_{x_0y_0} Y_0 = H_{xy}\left[P_{y_0y_0} - P_{mm}\right] P^{-1}_{y_0y_0} Y_0 \tag{2}$$

$$P_{\hat{e}\hat{e}} = \left[H_{xy}(P_{y_0y_0} - P_{mm}) - \hat{H}_{x_0y_0}P_{y_0y_0}\right](H^{*T}_{xy} - \hat{H}^{*T}_{x_0y_0}) + \hat{H}_{x_0y_0}P_{mm}H^{*T}_{xy} \tag{3}$$

where $\hat{X}_0$ is the spectrum of the combined solution; Y_0 is the input observation spectrum, m is the input error spectrum; H_{xy} is the theoretical frequency operator that connects the pure input y (the pure inputs are N_{grav} with KMS01; N_{grav} with KMS02; and N_{alt}) and the output signal X, that can be either N_{comb} (KMS01) or N_{comb} (KMS02); $\hat{H}_{x_0y_0}$ is the optimum frequency impulse response function; $P_{y_0y_0}$ is the input observation PSD; and P_{mm} is the input noise PSD.

Table 6 shows the statistics of the altimetric geoid, the gravimetric geoid with KMS01 and with KMS02 and the MIMOST combined solutions in the inner area.

Table 6. Statistics of the geoid models in the inner area [m]

	Min	Max	Mean	σ
N_{alt}	0.794	14.663	10.246	±3.279
N_{grav} with KMS01	1.079	14.715	10.201	±3.088
N_{grav} with KMS02	1.076	14.722	10.202	±3.087
N_{comb} (KMS01)	0.788	14.618	10.247	±3.278
N_{comb} (KMS02)	0.785	14.618	10.247	±3.278

3. Validation of the estimated geoid models

For the validation of the estimated geoid solutions, the stacked T/P SSHs were used together with the previous geoid models computed with EGM96 (Tocho et al., 2005). T/P provides repeated observations over the same tracks approximately every 10 days. The T/P SSHs data was used for the comparisons since they are known for their high accuracy and they are close to the geoid dataset because the sea surface variability present in the SSHs have been reduced during the stack process. The differences between stacked SSHs from the 3rd year of the T/P mission and the estimated geoid models were computed. All possible datum inconsistencies and systematic distortions on the data were minimized using a four-parameter similarity transformation model, as (Heiskanen and Moritz, 1967):

$$N^{T/P} = N^i - b_0 \cos\varphi \cos\lambda - b_1 \cos\varphi \sin\lambda - b_2 \sin\varphi - b_3 \quad (4)$$

where $N^{T/P}$ is the stacked T/P SSH, N^i is a gravimetric, altimetric or combined geoid height depending on the solution under consideration, and the parameters b_0, b_1, b_2 and b_3 were calculated using a least squares technique.

Also comparisons were performed using a 3rd order polynomial model referred to the multiple regression equation (MRE) (Fotopoulos, 2003):

$$N^{T/P} = N^i - \sum_{m=0}^{M} \sum_{n=0}^{N} (\varphi - \varphi_0)^n (\lambda - \lambda_0)^m x_q \quad (5)$$

where φ_0, λ_0 are the mean values of latitude and longitude of the T/P SSHs, and x_q contains the q unknown coefficients; q varies according to the number of terms up to a maximum of $q = (N + 1)(M + 1)$.

Those models are used in the same sense as in the terrestrial case when adjusting GPS/levelling geoid heights with gravimetric geoid solutions. It was assumed that a four-parameter model or a third order polynomial model can describe actual differences between T/P and geoid models developed; the differences were treated as they are due to the use of different datum in T/P and geoid models developed. From the results shown in Table 7, one can conclude that the use of a 3rd order polynomial model is preferable as compared to that of the use of four-parameter transformation.

Table 7. Geoid height differences between the estimated models and T/P SSHs in the inner area [m] (before and after removing bias and tilt fit)

	Min	Max	Mean	σ
N_{alt} – T/P SSHs	−1.15	1.15	0.15	±0.20
After a 3rd order polynomial model	−1.06	1.20	0.00	±0.19
After a four-parameter similarity transformation model	−1.21	1.09	0.00	±0.20
N_{grav} (KMS01) – T/P SSHs	−0.66	1.05	0.20	±0.28
After a 3rd order polynomial model	−0.80	0.85	0.00	±0.21
After a four-parameter similarity transformation model	−1.18	0.57	0.00	±0.23
N_{grav} (KMS02) – T/P SSHs	−0.67	1.05	0.20	±0.28
After a 3rd order polynomial model	−0.80	0.84	0.00	±0.21
After a four-parameter similarity transformation model	−1.19	0.57	0.00	±0.23
N_{comb} (KMS01) – T/P SSHs	−1.16	1.11	0.15	±0.20
After a 3rd order polynomial model	−1.04	1.18	0.00	±0.19
After a four-parameter similarity transformation model	−1.20	1.05	0.00	±0.20
N_{comb} (KMS02) – T/P SSHs	−1.16	1.11	0.15	±0.20
After a 3rd order polynomial model	−1.04	1.18	0.00	±0.19
After a four-parameter similarity transformation model	−1.20	1.05	0.00	±0.20

The results obtained indicate that the gravimetric geoid solutions computed using either KMS01 or KMS02 gravity anomalies do not differ. This is also reflected in the results of the combined solutions obtained using the MIMOST method. The altimetric geoid and the combined solutions exhibit the same differences with respect to the T/P SSHs.

The combined solution also improves the pure gravimetric solution by about 2 cm in terms of standard deviations of the differences with stacked T/P SSHs.

Figure 3 illustrates the MIMOST combined solution for the investigated area, calculated using the residual gravimetric geoid filled in with KMS01 data, as it is the same data used to derive the oldest solution computed with EGM96.

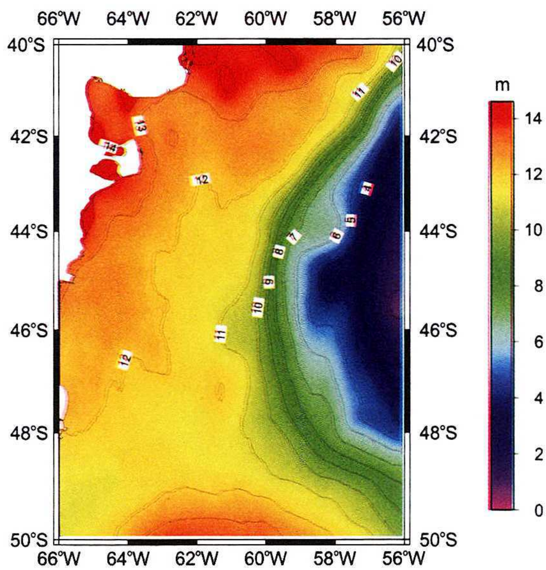

Fig. 3. The MIMOST solution

The results given in Table 8, and the comparisons made with the older solutions computed with EGM96 geopotential model (Tocho et al., 2005) and the T/P SSHs for the same area, show that the use of the new "combined" EGMs improves the results in terms of standard deviation by ± 1 cm, ± 2 cm, and ± 3 cm, for the pure altimetric solutions, pure gravimetric solutions, and the combined solutions, respectively.

Table 8. Geoid height differences between the estimated models and T/P SSHs in the inner area, calculated with EGM96 [m] (after removing bias and tilt fit, using a 3rd order polynomial model)

EGM96	Min	Max	Mean	σ
N_{alt} – T/P SSHs	−1.07	1.11	0.00	±0.20
N_{grav} – T/P SSHs	−1.00	1.35	0.00	±0.23
N_{comb} – T/P SSHs	−0.80	1.39	0.00	±0.22

It is worth mentioning, that the standard deviation of the differences for the comparisons with the altimetric models is quite high, at the ± 20 cm level, while a value close to ± 9 cm would be expected on the basis of previous studies (Li and Sideris, 1997; Vergos, 2002). The largest and smallest differences correspond to the points close to the coastline and in an area where the effect of the SSV is very high. Standard deviations of the differences were reduced to about ± 5 cm, and to ± 9 cm when some T/P SSHs points were omitted. The same improvement was achieved for the gravimetric and combined models. It can be concluded that by only stacking the T/P data the effect of the SSV cannot be completely removed so the SSHs are not representative to make comparisons. Perhaps, the T/P data has to be low-pass filtered in their along-track direction to remove the remaining oceanic effect.

4. Conclusions

Having determined a pure altimetric geoid model and gravimetric geoid height solutions for the Atlantic coastal region of Argentina, a combined solution using MIMOST method has been computed for a reduced area. The MIMOST method used for the optimal combination of heterogeneous data improves by ±2 cm the gravimetric only geoid model. The comparison with the old solution computed with EGM96 improves the results by ± 1 cm, ± 2 cm, and ± 3 cm for the altimetric geoid model, gravimetric solutions, and the combined solutions, respectively. This indicates that the new EGM is slightly better as a reference field used than EGM96 geopotential model.

For the determination of the optimal marine geoid model in the investigated area, a detailed analysis of the combination of land and marine gravity data on the coastline has to be carried out.

Acknowledgements

The authors wish to thank the Bureau Gravimétrique International for providing the shipborne data. We would like to thank the Editor, Prof. Jan Krynski, for his constructive comments, and the two reviewers for their time taken to consider this manuscript.

References

Andersen O.B., Knudsen P., (1998): *Global gravity field from ERS1 and Geosat geodetic mission altimetry*, Journal of Geophysical Research, Vol. 103, No C4, pp. 8129-8137.

Andersen O.B., Knudsen P., Trimmer R., (2005): *Improved high-resolution altimetric gravity field mapping (KMS02 Global marine gravity field)*, IAG Symposia, Vol. 128, F. Sanso (ed.), Springer. Proceedings of the Symposium 128: A window on the future of Geodesy, Sapporo, Japan, 30 June – 11 July 2003, pp. 326-331.

Andritsanos V.D., Tziavos I.N., (2002): *Estimation of gravity field parameters by a multiple input/output system*, Physics and Chemistry of the Earth, Part A, Vol. 25, No 1, pp. 39-46.

AVISO User Handbook, (1998): *Corrected Sea Surface Heights (CORSSHs)*, AVI-NT-011-311-CN, Edition 3.1.

BGI, (2001): Personal communication.

Dahl O.C., Forsberg R., (1998): *Geoid models around Sognefjord using depth data*, Journal of Geodesy, Vol. 72, pp. 547-556.

Forsberg R., (1984): *A study of terrain corrections, density anomalies and geophysical inversion methods in gravity field modeling*, Report of the Department of Geodetic Science and Surveying No. 355, The Ohio State University, Columbus, Ohio.

Fotopoulos G., (2003): *An analysis on the optimal combination of geoid, orthometric and ellipsoidal height data*, PhD. Thesis, University of Calgary, Department of Geomatics Engineering, UCGE Reports Number 20185.

Heiskanen W.A., Moritz H., (1967): *Physical Geodesy*, W.H. Freeman, San Francisco.

Lemoine F.G., Kenyon S.C., Factim J.K., Trimmer R.G., Pavlis N.K., Chinn D.S., Cox C.M., Klosko S.M., Luthcke S.B., Torrence M.H., Wang Y.M., Williamson R.G., Pavlis E.C., Rapp R.H., Olson T.R., (1998): *The development of the joint NASA GSFC and the National Imagery and Mapping Agency (NIMA) Geopotential Model EGM96*, Pub. Goddard Space Flight Center.

Li J., Sideris M.G., (1997): *Marine gravity and geoid determination by optimal combination of satellite altimetry and shipborne gravimetry data*, Journal of Geodesy, Vol. 71, pp. 209-216.

Li Y.C., (1993): *HFTGVBP Software package for the solution of GVBP by means of fast Hartley/Fourier Transform, TOPOGEOP Software packages to evaluate the TOPOgraphic effects on GEOdetic/GEOPhysical Observation*, Department of Geomatics Engineering, University of Calgary.

Sideris M.G., (1996): *On the use of heterogeneous noisy data in spectral gravity field modeling methods*, Journal of Geodesy, Vol. 70, pp. 470-479.

Smith W.H.F., Sandwell D.T., (1997): *Global Sea Floor Topography from Satellite Altimetry and Ship Depth Soundings*, Science Magazine, Vol. 277, Issue 5334.

Strang van Hees G., (1990): *Stokes' formula using fast Fourier techniques*, Manuscripta Geodaetica, Vol. 15, pp. 235-239.

Tocho C., Vergos G.S., Sideris M.G., (2005): *Optimal marine geoid determination in the Atlantic coastal region of Argentina*, In: F. Sansó (ed.) IAG Symposia, Vol. 128, "A Window on the Future of Geodesy", Springer – Verlag Berlin Heidelberg, pp. 380-385.

Tscherning C.C., Forsberg R., Knudsen P., (1992): *The GRAVSOFT package for geoid determination*, In: P. Holota, M. Vermeer (eds.), 1st Continental Workshop on the Geoid in Europe, Prague, 7-9 June 1993, pp. 327-334.

Vergos G.S., (2002): *Sea Surface Topography, Bathymetry and Marine Gravity Field Modeling*, MSc. Theses Dissertation, Dept of Geomatics Engineering, University of Calgary, UCGE Reports 20157, Calgary, Alberta.

Vergos G.S., Tziavos I.N., Sideris M.G., (2004): *On the validation of CHAMP- and GRACE-type EGMs and the construction of a combined model*, Presented at the Joint CHAMP/GRACE Science Meeting, 6-8 July, Potsdam, Germany.

Vergos G.S., Tziavos I.N., Andritsanos V.D., (2005a): *On the Determination of Marine Geoid Models by Least Squares Collocation and Spectral Methods Using Heterogeneous Data*, In: F. Sansó (ed.) IAG Symposia, Vol. 128, "A Window on the Future of Geodesy", Springer – Verlag Berlin Heidelberg, pp. 332-337.

Vergos G.S., Tziavos I.N., Andritsanos V.D., (2005b): *Gravity Data Base Generation and Geoid Model Estimation Using Heterogeneous Data*, In: C. Jekeli, L. Bastos, J. Fernandes (eds.) IAG Symposia, Vol. 129, "Gravity Geoid and Space Missions 2004", Springer – Verlag Berlin Heidelberg, pp. 155-160.

Wessel P., Smith W.H.F., (1998): *New improved version of The Generic Mapping Tools released*, EOS Transactions, Vol. 79, No 47, pp. 579.

Nowy model morskiej geoidy dla Argentyny, utworzony przy użyciu kombinacji danych altimetrycznych, morskich danych grawimetrycznych oraz modeli geopotencjału wyznaczonych na podstawie danych z misji CHAMP i GRACE

Claudia Tocho [1], Georgios S. Vergos [2], Michael G. Sideris [3]

[1] Wydział Astronomii i Geofizyki
Paseo del Bosque s/n, 1900 La Plata, Argentina
e-mail: ctocho@fcaglp.unlp.edu.ar
[2] Wydział Geodezji i Miernictwa, Uniwersytet Arystotelesa w Salonikach
Univ. Box. 440, 54124 Thessaloniki, Greece
e-mail: vergos@topo.auth.gr
[3] Wydział Inżynierii Geomatycznej, Uniwersytet w Calgary
2500 University Drive N.W., Calgary, Alberta, T2N 1N4, Canada
e-mail: sideris@ucalgary.ca

Streszczenie

Z modelowaniem geoidy morskiej na obszarze Atlantyku w pobliżu wybrzeży Argentyny wiąże się wiele problemów. Po pierwsze, brak wystarczającej ilości morskich danych grawimetrycznych uniemożliwia

modelowanie na tym obszarze czysto grawimetrycznej geoidy. Z drugiej strony, występowanie w tym rejonie bardzo silnych prądów oceanicznych zakłóca dane altimetryczne; czysto altimetryczny model geoidy jest obarczony zbyt dużym szumem, nawet po zastosowaniu wysokości poziomu morza (SSHs), przefiltrowanych przy użyciu nisko-pasmowego filtru, do usunięcia (częściowego) wpływu sygnałów oceanograficznych.

Proponowane kombinowane rozwiązanie polega zatem na łącznym wykorzystaniu wszystkich dostępnych danych grawimetrycznych i altimetrycznych. Zastosowana w nim kombinacja metod takich jak metoda kollokacji i teoria wejścia-wyjścia systemów (IOST) umożliwia filtrowanie danych przy użyciu nisko-pasmowego filtru oraz ich odpowiednie wagowanie. W rozwiązaniu tym wykorzystywane są także dane altimetryczne do wypełnienia luk w morskich danych grawimetrycznych.

Wszystkie dostępne morskie dane grawimetryczne, dane altimetryczne (SSHs) i najnowsze modele geopotencjału wyznaczone z wykorzystaniem danych z misji CHAMP i GRACE zostały użyte do wyznaczenia czysto altimetrycznego, grawimetrycznego i kombinowanego (z użyciem metody IOST) modeli geoidy morskiej dla Argentyny. Nowe modele geopotencjału, odgrywają istotną rolę w podniesieniu jakości modeli geoidy, w szczególności w odniesieniu do modelu EGM96, który był wykorzystany przy opracowaniu poprzedniego modelu geoidy morskiej na tym samym obszarze przy wykorzystaniu jedynie danych altimetrycznych z satelity ERS1. Z porównania opracowanych przez autorów modeli geoidy z SSHs otrzymanymi z misji TOPEX/Poseidon wynika, że modele altimetryczne charakteryzują się najlepszą zgodnością, zaś model kombinowany charakteryzuje się większą dokładnością aniżeli model czysto grawimetryczny.